# Polyatomic molecules in strong laser fields: Nonadiabatic multielectron dynamics

M. Lezius,[a] V. Blanchet,[b] Misha Yu. Ivanov, and Albert Stolow[c]
*Steacie Institute for Molecular Sciences, National Research Council of Canada, 100 Sussex Dr., Ottawa, Ontario K1A 0R6 Canada*

(Received 17 October 2001; accepted 1 May 2002)

We report the observation and characterization of a new nonresonant strong field ionization mechanism in polyatomic molecules: Nonadiabatic multi-electron (NME) dynamics. The strong field response of a given molecule depends on important properties such as molecular geometry and bonding, the path length of delocalized electrons and/or ionization potential as well as on basic laser pulse parameters such as wavelength and intensity. Popular quasi-static tunnelling models of strong field molecular ionization, based upon the adiabatic response of a single active electron, are demonstrated to be inadequate when electron delocalization is important. The NME ionization mechanism greatly affects molecular ionization, its fragmentation and its energetics. In addition, multi-electron effects are shown to be present even in the adiabatic long wavelength limit. © *2002 American Institute of Physics.* [DOI: 10.1063/1.1487823]

## I. INTRODUCTION

Electric forces underlie almost all of chemistry. Precise manipulation with strong external electric fields might, therefore, seem a natural choice for exploring the control of molecular dynamics. Laser fields in particular can be chosen strong enough to modify the potential energy surfaces which govern molecular dynamics. This goal appears increasingly within reach due to femtosecond laser technologies which permit the production of very high power, well-characterized yet variable coherent optical wave forms.[1–4] Modern amplified fs laser systems can easily produce focused intensities in excess of $10^{15}$ W/cm$^2$, corresponding to electric fields comparable to or stronger than the atomic Coulomb fields ($\sim 10^9$ V/cm) which bind matter itself. Indeed, strong field optical processes in atoms such as tunnel ionization and the generation of ultrahigh harmonics[5–7] are now routinely observed in many laboratories. The ability to apply these strong electric forces with high precision and little energy has lead to various applications in science and technology. For example, intense fs lasers have found their way as novel ionization sources in mass spectrometry.[8] There is also broad interest in the fs laser machining[9] of materials due to the high precision and significantly reduced local heat deposition of this process. In particular, the fs modification of transparent dielectrics promises to be a powerful method for writing integrated optical circuitry.[10]

Intense laser fields are playing an increasingly important role in molecular dynamics. Strong laser field control experiments have recently demonstrated that, using pulse-shaping techniques which adjust the phases of all colors within the laser bandwidth, bonds in polyatomic molecules can be selectively broken[11] and new bonds can be selectively formed.[12] The exact physical mechanisms which underlie this control presently remain unclear. Another area under investigation is in optical Coulomb explosion imaging which may emerge as a way of resolving the structural dynamics of polyatomic molecules.[13] However, recent experiments on diatomic molecules showed that very short pulses[14] can lead to strong electronic excitations in highly charged molecular ions, making it more difficult to resolve the time-dependent structure in such studies. The physical origins of these excitations are yet to be fully elucidated.

We shall be primarily concerned here with the electronic response of polyatomic molecules to intense nonresonant (infrared) laser pulses. Molecular systems often contain complex electronic structures. A fundamental question is: If many electrons are present, which ones are most strongly affected by the applied field and, therefore, would contribute most to any control schemes? When does the single active electron dynamics which dominates the strong field response of atoms give way to a richer multielectron response expected in molecules? It is the purpose of the present work to elucidate some of this complexity and to discuss important limiting cases which arise when strong laser fields are applied to polyatomic molecules.

In addressing these questions, we begin by reviewing the current understanding of strong-field interactions in atoms and small molecules, focusing on the underlying physical assumptions and their limits. There has been outstanding success in describing the detailed behavior of atoms in strong infrared laser fields.[15–19] A simple physical picture has emerged whereby, for sufficiently long wavelengths, the strong field ionization of atoms is described by the tunnelling of the most weakly bound electron (of binding energy $I_p$) through an essentially static barrier formed by the superposition of the core potential (Coulomb electric field) with the laser electric field. This static picture emerges when the elec-

[a]Also at: Universität Innsbruck, Institut für Ionenphysik, Technikerstr. 25, A-6020 Innsbruck
[b]Also at: Université Paul Sabatier, IRSAMC 118 Route de Narbonne, 31400 Toulouse, France
[c]Electronic mail: albert.stolow@nrc.ca

 

tron can tunnel very quickly as compared to the time scale for the barrier to reverse (i.e., the laser period). This physical idea rests upon both the quasi-static and single active electron (SAE) approximations, discussed in more detail below. These in essence amount to: (i) Ignoring any electron excitation inside the potential well, based upon an adiabatic approximation; and (ii) ignoring any multi-electron effects. The quasi-static SAE picture has been extremely successful in atoms[15,16] and small molecules[20] when the so-called Keldysh parameter[21] is small: $\gamma \ll 1$ (in practice $\gamma < 0.5$). The Keldysh parameter, discussed in more detail below, is related to the ratio of the tunneling time $\tau_t = \sqrt{2I_p}/\epsilon$ to the laser period $\omega_L^{-1}$ and can be defined as:[21] $\gamma = \tau_t \omega_L$. When the tunneling time is short compared to the laser period, we can consider the tunneling probability as varying parametrically with the amplitude of the applied strong field. As the tunnelling probability varies exponentially with barrier suppression, essentially all tunnelling events occur at the turning points (i.e., maximal barrier suppression) of the field oscillation. It is for this reason that a purely static calculation of the tunneling rates is successful.

Where and when should these two main approximations break down? The adiabatic approximation assumes that the time scale of electron motion inside the potential well is much faster than the laser period: The electrons are assumed to adjust instantaneously to the time-varying electric field $\mathcal{E}(t)$ of the laser. This is completely analogous to the familiar Born–Oppenheimer approximation where the time scale of electron motion is assumed to be much faster than that of the time varying electric field due to nuclear motion. The commonly used figure of merit in strong field ionization studies is the Keldysh tunneling parameter. While the original Keldysh theory[21] is not limited to tunnelling, it was derived for a zero-range potential and is, therefore, intrinsically unable to account for any electron dynamics inside the potential well. Therefore, the limit $\gamma \ll 1$ should not be identified with the adiabaticity of the electronic response: The Keldysh parameter relates only to the electron motion under the (tunnelling) potential barrier and completely ignores any electron dynamics inside the well. Other Keldysh type approaches[22,23] suffer from this same drawback. This concern applies equally to the theory developed by Perelomov, Popov, and co-workers[24] and its tunneling limit of $\gamma \ll 1$ derived by Ammosov, Delone, and Krainov,[25] now commonly called ADK theory. For single ionization of atoms close to threshold, it is generally accepted that ADK is highly successful. These theories include corrections to account for the proper Coulombic shape of the binding potential but still (implicitly or explicitly) use the quasi-static (i.e., adiabatic) approximation for the electron dynamics inside the potential well.

The adiabatic approximation is justified in rare gas atoms because the time it takes for an electron to ''traverse the atom'' is typically subfemtosecond, much less than the laser period. This approximation will inevitably fail when the time scale of electron dynamics within its associated potential approaches the laser frequency, as can be the case in polyatomic molecules.

The second standard approximation in the strong-field atomic physics is the single active electron (SAE) approximation. The SAE picture should fail when multiple electrons which can *effectively* respond to the laser field (and interact with each other) are present in the potential. The simplest type of multi-electron phenomena are the correlation effects observed in multiphoton double ionization processes[26] which originate from rescattering phenomena and autoionizing resonances.[27] Nevertheless, for single ionization of atoms it has been commonly accepted that the SAE approximation is justified unless resonances with bound two-electron excited states are explicitly involved. SAE response is indeed the case in rare gas atoms: Even though they have multiple equivalent electrons in their outer shell, all doubly excited states which can contribute to the strong field polarizability are well above the ionization potential. The neglect of other electrons and, hence, the couplings between them greatly simplifies the problem. For He, Ne, Ar, and Xe, SAE calculations[18,28] yield outstanding agreement with experiments.[15,16,19]

In the strong field ionization of small molecules, the vibrational time scale has to be compared to the pulse duration and, in extreme cases, to the laser period itself. For example, in $H_2$ and in CH bonds the vibrational time scale is about 10 fs, shorter than the duration of most femtosecond pulses. Benchmark calculations of ionization rates of simple molecules such as $H_2^+$, $H_2$, and $H_3^+$ show that the ionization rates at intensities of $I \sim 10^{15}$ W/cm$^2$ can approach 10 fs.[29] In such cases the electronic and vibrational responses may be nonseparable. In particular, even for short (few tens of femtoseconds) pulses interacting with larger organic molecules, a question will be whether or not the CH bonds are strongly coupled to the driven electron dynamics.

The additional aspect of vibrational dynamics leads to a number of important, qualitatively new effects. If large-amplitude vibrational dynamics is present during the laser pulse, a new ionization mechanism obtains. When the bond is stretched to a certain critical length $R_c$, which is typically significantly greater than the equilibrium bond length, efficient multiple ionization occurs.[30–35] This phenomenon of ''enhanced ionization'' has been extensively investigated for diatomic and small polyatomic molecules, see, e.g., Refs. 30–35.

For $H_2^+$, exact numerical simulations[31] have shown that the maximum in the ionization rate occurs when the lowest unoccupied molecular orbital (LUMO) is Stark-shifted by the instantaneous electric field of the laser to just above the Coulomb barrier for the electronic motion. However, the LUMO, which acts as a doorway to ionization, must in addition be populated in order to enable this mechanism. This is achieved when the electronic response to the laser field oscillation becomes nonadiabatic. As the $H_2^+$ bond stretches, the highest occupied molecular orbital (HOMO)–LUMO coupling increases and the field-free energy gap decreases, both leading to a nonadiabatic electron response with respect to the laser oscillation, thus populating the LUMO. In other molecular systems the LUMO may not be the doorway state to ionization: In $H_2$ the relevant doorway states are the ion-pair states.[33]

For sufficiently large $R \geqslant R_c$, the same phenomenon can

be described using an atomic picture.[30] The coherent superposition of HOMO and LUMO, due to the nonadiabatic electron response, corresponds to a dynamic electron localization at one of the atoms. The tunnelling barrier at this atomic core, suppressed by the laser field, is additionally suppressed by the Coulomb field of the other atomic core, leading to a greatly enhanced ionization rate.[30]

We stress that population of the doorway states need not be resonant. This is confirmed by calculations[31] showing that the enhancement structure in the ionization rate is associated with conditions for dynamic electron localization (via nonadiabatic population of the Stark-shifted LUMO) and not with multiphoton transitions that become resonant at certain values of the internuclear distance $R$.

It is very important to note that the contribution of this enhanced ionization to strong field molecular ionization depends greatly on the pulse duration. If the pulses are too short, vibrational excursions cannot reach $R_c$ before the field turns off and enhanced ionization will be absent. If the pulses are longer than the time required to reach $R_c$, then essentially all ionization events will occur at $R_c$. [As discussed in a following section, we specifically used short 40 fs pulses in the present study in order to minimize effects associated with enhanced ionization. We also kept intensities relatively low in order to avoid strong multiple ionization followed by the Coulomb explosion, resulting in significant fragment ion energies[36] and fast nuclear motions (significant even on 40 fs time scale).]

As the system size increases from diatomic to polyatomic molecules and clusters, the situation changes again. The zero-length scale approximation in the quasi-static tunneling model was revised by showing that a longer molecule intrinsically leads to a lowering of the barrier,[37] as observed in the shape of the photoelectron spectra of field-ionized molecules. A ''correction'' to the Keldysh parameter which accounts for the molecular ''length'' has been developed.[37] In the following, we will call this ''length-corrected'' quasi-static model, the molecular single active electron (MSAE) picture.

The MSAE model suggests that the larger the system, the more readily the tunneling limit obtains as compared to an atom of similar ionization potential $I_p$: The larger the molecule, the more efficient the strong-field ionization. Recent experiments,[38] however, suggest the opposite trend: The intensity thresholds for efficient strong-field ionization, measured for a large number of polyatomic molecules, are higher than those for atoms of similar $I_p$. Our experiments reported here confirm this trend, and the numerical simulations described in the following section suggest that the origin of these higher ionization thresholds lies in strong field-induced polarization of all delocalized electrons, even in the low-frequency limit.

As systems increase further in size, collective multielectron behavior should start to dominate their strong-field response. Experimental studies on fullerenes[39–42] and molecular,[43] metallic,[44] and rare-gas[45–50] clusters revealed a number of interesting phenomena: High ion kinetic energies,[45,48] efficient ionization rates,[49] extreme ultraviolet (XUV) photon,[46] and x-ray generation,[47] rapid fragmentation, and high electron kinetic energies with multiple energy distributions.[50] For these larger aggregates, a ''nano''-plasma-based description appears appropriate.[48,51] The question one would like to address is: What degree of system complexity is necessary to induce the transition from single to multiple electron dynamics in strong, low-frequency fields? Our model calculations suggest that the onset of plasma-like multielectron behavior could be related to fast saturation of nonresonant Landau–Zener-type electronic transitions between the ground and excited electronic states, as discussed in detail below.

In a recent letter,[52] we reported our observation and characterization of a new, general type of nonresonant strong laser field ionization which can exist in polyatomic molecules: Nonadiabatic multi-electron (NME) dynamics. In the following, we present a full account of this work, including additional experimental results and a simple physical model which illustrates the essential physics.

This paper is organized as follows. We begin with a very simple driven electron-in-a-box model in order to motivate the discussion and to illustrate the physical phenomena of concern here. We then describe our experimental methods for making the calibrated, absolute intensity measurements which were important in this study. In order to address the potential failure of the adiabatic and SAE approximations in polyatomic molecules, we report our studies on unsaturated hydrocarbons (the linear polyenes), which have many delocalized $\pi$ electrons. Through systematic variation of the length of the polyene and by studying its ionization and fragmentation patterns as a function of wavelength (from 1500 to 400 nm), we observed the transition from quasi-static tunneling ionization to nonadiabatic multielectron behavior.

## II. PHYSICAL MOTIVATION: A DRIVEN ELECTRON-IN-A-BOX MODEL

A very simple model for picturing phenomena related to strong field ionization dynamics is based on a smooth one-dimensional (1D) particle-in-a-box potential, $U(x)$

$$U(x) = -U_0 \frac{1+\exp(-L/2a)}{1+\exp(|x|-L/2a)}. \tag{2.1}$$

We study both single and multiple electron laser-induced dynamics in this model potential. For the multiple active electron (MAE) situation, we borrow an approach used in cluster studies.[53] In the low-frequency limit, the main multi-electron effect is the significant change in the (quasi-static) self-consistent Coulomb field experienced by an electron due to the displaced density (i.e., polarization) of the multi-electron cloud. Within this approximation, each electron is self-consistently initialized in its corresponding field-free state (orbital) $\psi_n^{(0)}$ of the box. Each electron's dynamics is described by: (1) The effective one-electron field-free stationary potential $U(x)$ [in our case modelled by Eq. (2.1)], (2) the interaction with the laser field, and (3) the interaction with the *differential* Coulomb potential due to the laser-induced *displacement* of the total electron density $\Delta\rho$

$$\Delta\rho(x) = \sum_n \left(|\psi_n(x,t)|^2 - |\psi_n^{(0)}(x)|^2\right),$$

$$\Delta U(x) = \int \frac{\Delta\rho(x')}{\sqrt{(x-x')^2+a^2}}dx'. \tag{2.2}$$

Here $a$ is a standard smoothing parameter for one-dimensional simulations. In our simulations, we choose $a$, $L$, and $U_0$ to roughly reproduce the ionization potential and electronic level spacings of one of the linear polyenes (all-trans decatetraene) used in our experiments

$$\begin{pmatrix} U_0 = -7.1 \text{ eV} \\ L = 13.2 \text{ Å} \\ a = 3.6 \text{ a.u.} \end{pmatrix} \rightarrow \begin{pmatrix} E_4 = -7.1 \text{ eV} \\ E_3 = -8.6 \text{ eV} \\ E_2 = -9.8 \text{ eV} \\ E_1 = -11.7 \text{ eV} \end{pmatrix}. \tag{2.3}$$

Such a crude model lacks many aspects of MAE behavior and relies on the assumption that they are all included in the field-free effective potential $U(x)$ which in principle may contain any existing field-free electron correlations. We emphasize again that we use the *difference* in the self-consistent field (SCF)—Eq. (2.2). In spite of the highly simplified nature of our model, we expect that it will allow a qualitative understanding of the dynamics in the low-frequency limit where the change in the SCF is the dominant effect and should allow us to see the onset of the departure from the quasi-static dynamics.

Some of the results of these calculations are presented in Figs. 1 and 2. The simulation considered four pairs of $\pi$ SCF electrons, each pair occupying one orbital as per Pauli's principle. At time zero, before any field is applied, they have the expected nodal structure. Driven by the field, each electron starts to oscillate in the field and reacts to the displacement of the Coulomb field due to all other electrons. Although only the total electron density has a physical meaning in this model, it is instructive to observe the evolution of each initial orbital to verify that all electrons respond to the field [see Figs. 1(a)–1(d)].

An example of the time dependent evolution of a driven single active electron (SAE) is depicted in the top panel of Fig. 1, showing the SAE electron density as a function of time and coordinate. It evolves with increasing oscillations in $R$. When the density localizes close to the barrier, tunneling is observed. Outside the potential, the density is damped by an absorbing boundary. As the electric field strength increases, the electron oscillations increase in amplitude, eventually leading to ionization within about 1 1/2 optical cycles. Parts of the density are also scattered at the edges of the well, resulting in ''splash''-like excitation events.

At each laser wavelength $\lambda$ the total ionization probability $W_{\text{ion}}(I)$ was calculated as a function of laser intensity. A frequency-dependent saturation intensity $I_{\text{sat}}(\lambda)$ was defined as the limit when the probability of single or higher ionization is $W_{\text{ion}}(I) \approx 0.9$. For long wavelengths, the onset of ionization is very steep and $I_{\text{sat}}$ is not very sensitive to the exact form of $W_{\text{ion}}(I)$. As shown in Fig. 2, we observe a strong frequency dependence to the calculated $I_{\text{sat}}$, decreasing towards shorter wavelengths (higher frequencies). For long wavelengths, the $I_{\text{sat}}$ is higher for the many-electron case than for the single-electron case. We also show the results expected for the quasi-static atomic tunnelling (obtained via the ADK tunneling formula[25]) and the length-corrected molecular single active electron (MSAE) result.[37] Of course, due to their inherent adiabatic approximation, both the ADK and MSAE results are wavelength independent.

Our model shows that there are many-electron effects even in the low frequency adiabatic (quasi-static) limit, since the calculated $I_{\text{sat}}$ is higher for the many-electron case. We believe that the reason for this is a dynamic shielding effect caused by the higher polarizability of the multi-electron system. Simply put, the dynamic polarization of all *other* electrons in the field essentially pushes them towards the potential wall. This adds additional electron–electron Coulomb repulsion to the potential barrier, making it harder for the active electron to escape. The induced dipole moment, which will depend on the total number of delocalized electrons in the system, can partially negate the externally applied field and, therefore, increase the effective $I_{\text{sat}}$. This observation is consistent both with our experimental data (vide infra) and previous observations[38] and is currently under further investigation in our laboratory.

Very qualitatively, the electron density dynamics seen in our calculations suggest a rough analogy with the splashing of water in a periodically tipping bathtub of length $L$. In our case, it is the oscillating electric field that causes the potential to periodically tip left and right (at the laser frequency $\omega_L$), forcing the electron density to oscillate within the well. In the low frequency limit, the bathtub tips very slowly and the surface of the water remains flat at all times (adiabatic dynamics). As the amplitude (angle) of the tilt increases, water begins to pour over one edge or the other (tunnel ionization). Depending on the degree of tilt (laser intensity), more water may be lost (multiply charged cations) but the surface of the water always remains flat (no electronically excited cation states). If the time it takes for water to pour over the edge (classical analogue of the tunneling time) is much less than the time to reverse the tilt (laser period), then the ratio of these two times (the Keldysh parameter) is much less than unity. This corresponds to the standard quasi-static picture. Independent of this (Keldysh) ratio, if the frequency of the tipping motion now increases, the water no longer remains flat due to the formation of waves (nonadiabatic dynamics) and, as the amplitude increases, water is splashed out of the bathtub (nonadiabatic ionization dynamics). Furthermore, the waves can remain even after the tilting (laser) has been turned off (formation of electronically excited states which persist after the laser pulse is turned off). When the laser period matches the time scale of electron motion inside the potential well, there can be very large amplitude density oscillations.

The results of our calculations show that for increasing length (or, equivalently, decreasing level spacings), the excitation–ionization dynamics appeared to change from quasi-static tunneling to a ''splashing'' dynamical behavior. The latter effect could potentially result in large energy absorption, even at low intensities and in the absence of field-free resonances. The nonadiabatic departure from quasi-static tunneling can occur even when the Keldysh parameter $\gamma$ is less than unity, whether corrected or not for molecular size effects.[37] It is important to note that the Keldysh parameter relates only to the tunneling motion through the field-

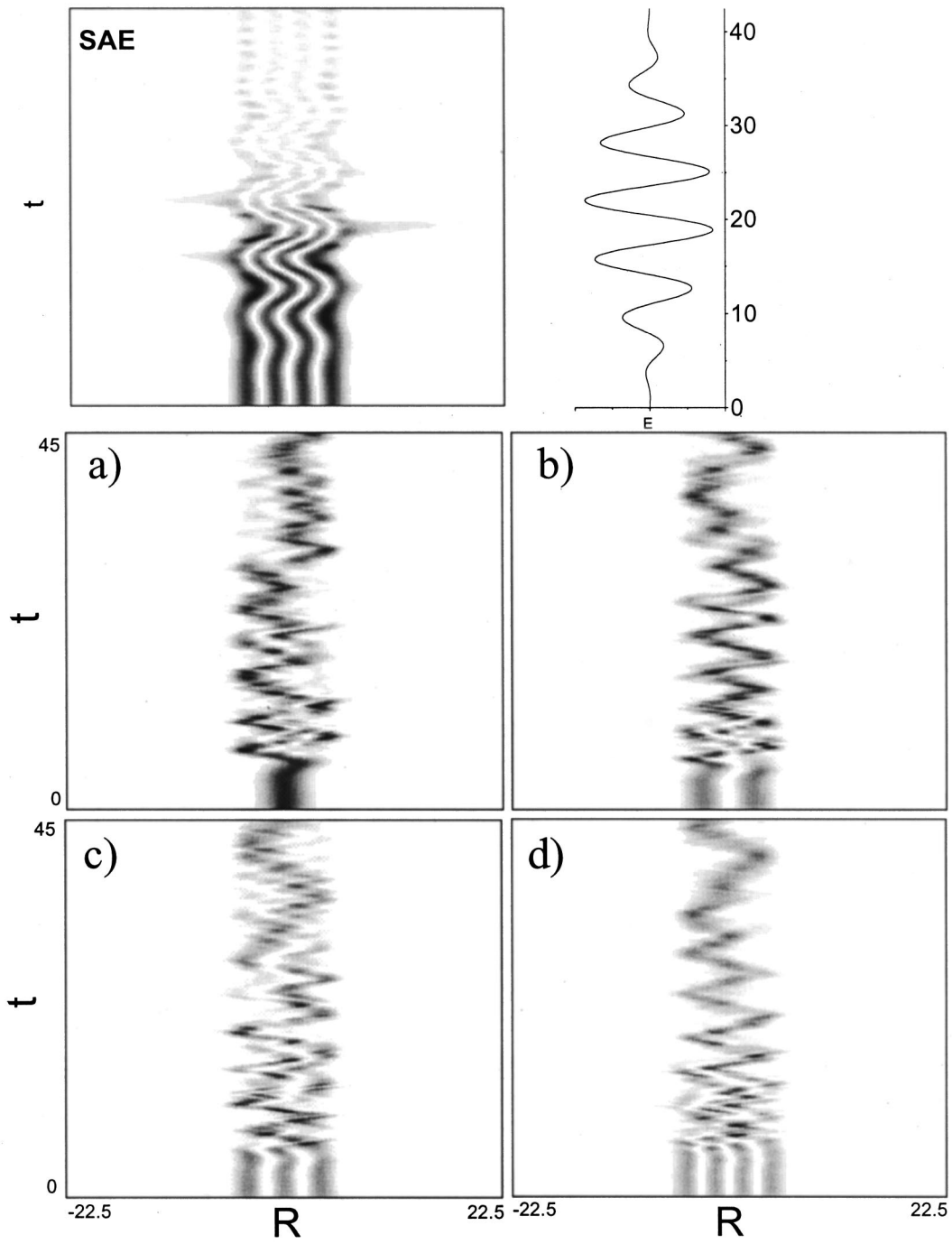


FIG. 1. Top: A $R-t$ probability density plot of a single active electron (SAE) in a 1D potential driven by a strong (40 fs) alternating electric field pulse (shown on the right). Ionization events occur at the fourth, fifth, and sixth half-cycle of the pulse. (a) A $R-t$ density plot showing the 40 fs time evolution of the first self-consistent field (SCF) coupled eigenstate in a 1D potential driven by the same field. (b)–(d) correspond to the second, third and fourth SCF eigenstates. While only the total density (sum of all four graphs) carries physical significance, it is important to note that all orbitals are strongly and nonlinearly affected by the electric field.

induced potential barrier and that it completely ignores any electron dynamics inside the well. We will further analyze, below, the results of our simulations and the qualitative physical picture that they suggest by using the Landau–Dykhne theory of nonadiabatic transitions.[54] We stress that here the term ''nonadiabatic'' refers to the driven electron motion with respect to the oscillations of the electric field during the laser cycle. This should not be confused with the non-Born–Oppenheimer coupling between the electronic and vibrational motions, which can also cause laser-assisted electronically nonadiabatic transitions between laser-induced potentials of the dressed molecule (see, e.g., review[55] and/or[56] for recent experiments).

The time scale of response in bound quantum systems is given by the inverse level spacings in the problem. If electronic level spacings are very large compared to the (near IR)

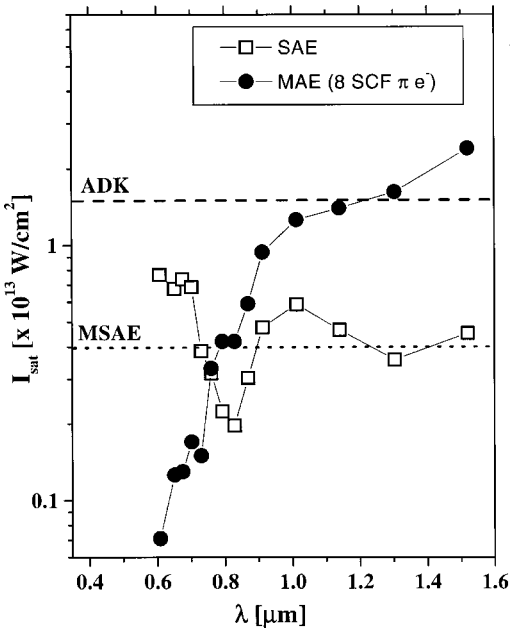


FIG. 2. Saturation thresholds $I_{\mathrm{sat}}$, defined as 90% ionization, as a function of wavelength obtained from simulations for a single active electron (SAE) and for multiple active electrons, MAE (eight SCF $\pi$ electrons). The eight SCF electrons initially populated the four lowest eigenstates of an electron-in-a-box-type potential (see text). Also indicated are the wavelength independent $I_{\mathrm{sat}}$ expected from molecular single active electron models (MSAE) and from ADK theory. For a discussion, see the text.

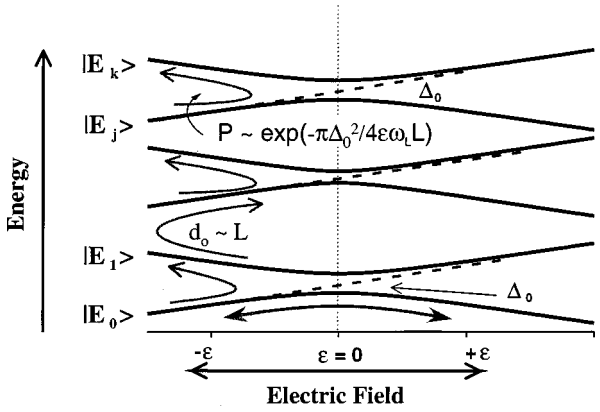


FIG. 3. Sketch of a one-dimensional multilevel quantum system of length $L$, average level spacing $\Delta_0$ and molecule transition dipole coupling $d_0$ in a strong oscillating electric field $\mathcal{E}$ of frequency $\omega_L$. In the adiabatic low frequency limit, all states Stark shift smoothly with $|\varepsilon|$ and the populations remain in their respective adiabatically field-dependent eigenstates. As the frequency increases, Landau–Zener-type nonadiabatic transitions can occur at the avoided crossings with probability $P$. Such nonadiabatic strong field transitions can lead to nonresonant excitation of many electronically excited states after only a few laser cycles.

photon energy, the electron can usually be considered to behave adiabatically with respect to field oscillations. This is indeed the case for rare-gas atoms. However, for molecules with delocalized orbitals, the electronic level spacings vary inversely with the ''length of the molecule'' and the adiabatic approximation can fail. If we allow for large amplitude nuclear dynamics, these types of nonadiabatic effects can be seen even in the simplest diatomic molecule $H_2^+$ where the efficiency of nonresonant electronic excitation and ionization depends greatly on the internuclear distance $R$.[31] In particular, stretching $R$ from the equilibrium to a critical distance $R_c \sim 4$ Å not only maximizes the ionization rate of the Stark shifted LUMO, but also greatly increases the probability of efficient nonresonant population of this state (which acts as the doorway to ionization). The efficiency of nonresonant, nonadiabatic $\sigma_g \rightarrow \sigma_u$ transition increases at large $R$ because the $\sigma_g \rightarrow \sigma_u$ coupling increases with $R$ and, simultaneously, the electronic energy gap decreases.

Our simulations show that nonadiabatic electron dynamics becomes increasingly more pronounced in polyatomic molecules with delocalized electrons as one increases the molecular size. While the exact conditions for the onset of efficient nonresonant population of the excited states will depend on the specific molecule, a Landau–Dykhne-type analysis[54] offers a simple semiquantitative estimate. Consider a system with characteristic length $L$ and field-free level spacing $\Delta_0$, subjected to an oscillating field $\mathcal{E} = \varepsilon \sin \omega t$. This situation is depicted in Fig. 3. For a laser frequency $\omega \ll \Delta_0$, the levels will shift via the Stark shift as the field increases towards $+\varepsilon$ or $-\varepsilon$. In the purely adiabatic limit, the populations always remains in their Stark shifted initial states without undergoing transitions to higher (or lower) lying states. However, as the laser frequency and/or the Stark shift increases, the system will oscillate more quickly between $+\varepsilon$ and $-\varepsilon$. (For sufficiently strong fields, the Stark shift will no longer be quadratic, but will rather scale with the voltage $\varepsilon L$ applied across the length of the molecule.) Landau–Zener type nonadiabatic transitions will become increasingly probable, allowing population to evolve towards higher-lying (bound) electronic states. This process will be highly efficient and virtually insensitive to resonances if these nonadiabatic transitions are saturated within a few laser cycles: This situation implies a great energy broadening of the manifold of electronically excited states and, thus, the formation of an electronic quasi-continuum.

For a pair of electronic states separated by $\Delta_0$ and coupled by the molecular dipole matrix element $\mu$, the probability $P_{\mathrm{LZ}}$ of nonresonant Landau–Zener-type nonadiabatic transitions during one-half a laser cycle is[54]

$$P_{\mathrm{LZ}} \sim \exp(-\pi \Delta_0^2 / 4 \omega_L \mathcal{E} \mu). \tag{2.4}$$

Several comments are required before we discuss applying this expression to molecular systems. First, it assumes that the nuclear motion is negligible during a one-half of a laser cycle. Second, the transition matrix element should be evaluated at the instantaneous molecular geometry: For very short pulses, the equilibrium geometry should provide a sufficiently accurate estimate. Finally, $\Delta_0$ and $\mu$ should be chosen to correspond to the states most strongly coupled to the ground state. In general, the value of the dipole matrix elements $\mu$ will increase with increasing $L$, as is certainly the case for charge-transfer and charge-resonant states, where $\mu$ scales as $L$.[57] Consequently, when $\omega_L \mathcal{E} L \sim \Delta_0^2$, transitions which correspond to charge transfer across the molecule become quickly saturated. This implies strong nonresonant absorption by *all* delocalized electrons involved in this coupling. (We note that for many polyatomic molecules, the relatively unpolarizable electrons associated with C–H

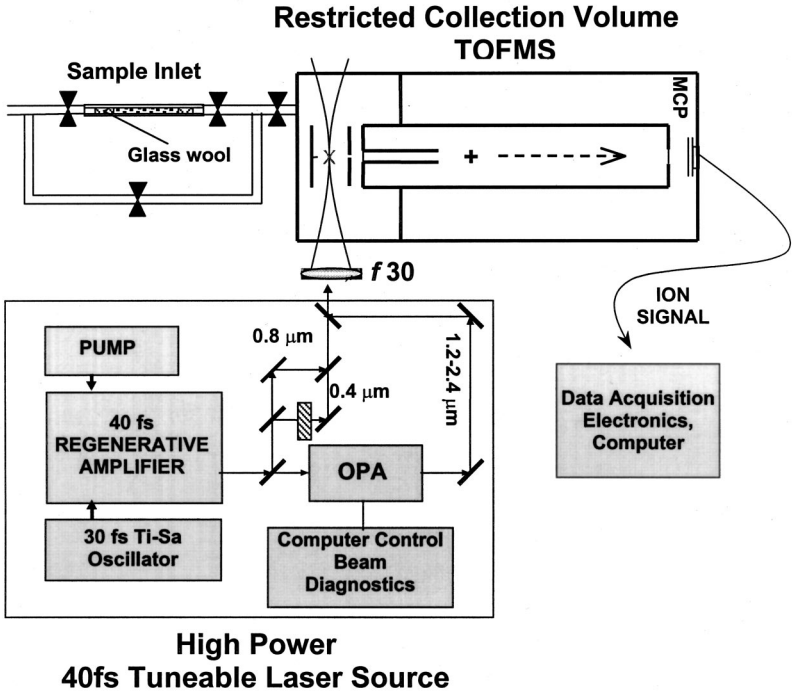


FIG. 4. A depiction of the experimental setup. A 0.8 $\mu$m 30 fs Ti:Sa oscillator is regeneratively amplified, yielding 40 fs, 700 $\mu$J pulses. These were either used directly or pumped a short pulse OPA system, producing high power (>100 $\mu$J) 40 fs pulses in the 1.2–2.4 $\mu$m range. A restricted collection volume time-of-flight mass spectrometer (TOFMS) ensured that ions were collected only from a cylindrical volume of constant axial intensity. Ion signals and laser pulse energies were recorded every shot. The sample inlet consisted of a glass wool reservoir from where molecules were evaporated at ambient temperature and transported in an inert carrier gas to the interaction region. For details, see the text.

bonds are not much involved in this charge-transfer or charge-resonant coupling, and therefore, the fact that their vibrational periods approach the period of infrared laser fields is of small import here.)

The atomic analogue of such a nonresonant nonadiabatic response has been described theoretically[58] and observed experimentally[59] in the strong field microwave ionization of atomic Rydberg states. In the MAE case, this represents a nonadiabatic multi-electron (NME) excitation mechanism which leads to a *complete* failure of both the adiabatic (quasi-static) and the SAE pictures. This failure is intrinsically independent of the nature of the barrier and can occur even when $\gamma<1$, a case which is formally considered the tunneling limit. It is important to note that the greater the length $L$, the easier it is to reach the limit $\omega_L \mathcal{E} L \sim \Delta_0^2$. As a specific example, with $L=13.5$ Å, $\Delta_0=4$ eV, and $\lambda=700$ nm, we find that $\omega_L \mathcal{E} L=\Delta_0^2$ already at an intensity $I \approx 5.6\times 10^{12}$ W/cm$^2$, a situation which corresponds to our experimental results on the polyene all-trans decatetraene (see next section) and, importantly, obtains in *many* strong field experiments on molecules.

The creation of an electronic quasi-continuum via extreme broadening of excited states through highly efficient nonadiabatic transitions suggests that the subsequent driven multi-electron dynamics might be qualitatively understood in terms of classical mechanics. From a classical perspective, the important classical parameters for electronic motion in the quasi-continuum are: (1) The electron oscillation amplitude $a_{\mathrm{osc}}=\mathcal{E}/\omega_L^2$ and (2) the length of the delocalized electron path inside the molecule $L$. There are two limiting cases: $a_{\mathrm{osc}} \gg L$ and $a_{\mathrm{osc}} \ll L$. Classically, when $a_{\mathrm{osc}} \gg L$ the electron is pushed by the field along the entire length of the molecule and then scatters (splashes) off the edge of the potential well (this occurs twice per full laser cycle). The energy typically absorbed (the work done on the electron) during each scattering event is $E_{\mathrm{scat}} \sim \mathcal{E} L$. When $E_{\mathrm{scat}}$ exceeds typical level spacings, electronically excited states are formed. When $E_{\mathrm{scat}}$ approaches the ionization potential $I_p$, these states will ionize over the barrier in the next optical half-cycle.

In the other limit of $a_{\mathrm{osc}} \ll L$, $E_{\mathrm{scat}} \sim U_p=\mathcal{E}^2/4\omega_L^2$, the average (ponderomotive) energy of electron oscillation in the laser field. Since the ponderomotive electron drifts as well as oscillates, it will soon hit the edges of the potential. When $I_p<U_p$, the atomic Keldysh parameter $\gamma=\sqrt{I_p/2U_p}$ is less than unity, a situation that is usually interpreted as tunnelling. However, ionization can now proceed via absorption of energy $\sim U_p$ in one scattering (splashing) event, once again followed by over-the-barrier escape during the next laser half-cycle. Such an ionization mechanism becomes the typical case with increasing box length $L$. We conclude this discussion by reiterating that the Keldysh parameter is not necessarily diagnostic of tunneling behavior.

## III. EXPERIMENT

The experimental arrangement, illustrated in Fig. 4, is described in detail elsewhere.[38] Briefly, a mode-locked Ti:Sapphire laser oscillator produced ≈30 fs pulses at 0.8 $\mu$m which were subsequently regeneratively chirped pulse amplified (CPA). The 30 nm bandwidth of the NRC-design CPA system maintained a compressed pulse duration of 40 fs while delivering 700 $\mu$J per pulse at a repetition rate of 330 Hz in a near diffraction-limited spatial mode. The 0.8 $\mu$m pulse was either used directly or it pumped a short-pulse, five-pass optical parametric amplifier (TOPAS), generating broadly tuneable (1.2–2.4 $\mu$m) high power infrared pulses of ≈40 fs duration. Additionally, via second harmonic generation in 0.1 mm BBO crystals, high power 40 fs pulses could be generated at 0.4 and 0.6–1.2 $\mu$m. These laser pulse characteristics were confirmed via autocorrelation, spectrometry

and frequency resolved optical gating (FROG). After variable attenuation, pulse energies were monitored on a shot-to-shot basis using an integrating sphere in order to bin the experimental data with respect to intensity (*vide infra*).

The central goal of this work was to study the intensity and wavelength dependence of strong field molecular ionization processes. Importantly, in these studies we specifically avoided the deleterious effects of spatial averaging over the length of the laser focus. The intense pulses were focused with achromatic f30 optics into the interaction region of a restricted collection volume time-of-flight mass spectrometer (TOFMS, resolution of 300). At 0.8 $\mu$m, the focusing geometry yielded a $R=27$ $\mu$m diameter beam waist and a Rayleigh range of 3 mm, as measured with a CCD camera beam profiling system. The entrance electrode to the TOFMS had a 500 $\mu$m slit aperture so that the Rayleigh range was significantly longer than the width of the aperture. This ensured that ionization events were collected only from a cylinder of constant axial intensity. The maximal Gaussian peak laser intensity $I_0$ was $2.7\times10^{15}$ W/cm$^2$. This was independently confirmed by studying the intensity dependence of helium ionization. Gaussian spatial behavior at the laser focus was further confirmed by scanning the focus with respect to the entrance slit to the TOFMS drift region. The laser polarization was directed along the TOFMS axis.

Low density gas, typically $10^{-6}$ Torr pressure in order to avoid space charge effects, was introduced to the ionization region through a variable leak valve. We introduced solid samples using a weak flow of a carrier gas (e.g., He) through a glass tube packed with pre-cleaned glass wool. The solid phase organic molecules used in these experiments (all-trans Decatetraene, $\beta$-Carotene) were dissolved in hexane and evaporated on the glass wool before use, thus yielding a huge exposed surface area. For the liquid phase organic molecules used in these experiments (trans-Hexatriene and Cyclooctatetreaene), the vapor pressure was sufficiently high so as to not require this carrier gas technique. In all experiments, we avoided heating the samples in order to eliminate any risk of thermal decomposition. A large aperture TOFMS, described previously,[60] was used to determine the kinetic energy release amongst the ionization fragments. Again, the laser polarization was directed along the TOFMS axis. For all kinetic ions observed here, the 0.75″ aperture was nonvignetting. Experiments consisted of measuring mass spectra as a function of laser pulse energy, via variation of an attenuator. At each wavelength, laser pulse characteristics were determined and the energy scans repeated. The energy scans were converted to calibrated absolute laser intensity scans, described below.

As discussed in detail by Hankin *et al.*,[38] a cylindrical ionization volume of constant axial intensity allows for the development of calibrated absolute intensity measurements through the definition of the saturation intensity $I_{\mathrm{sat}}$. We have used this method to make precise and accurate intensity measurements as a function of wavelength. The ionization signal produced by a parallel Gaussian beam of peak intensity $I_0$ is given by

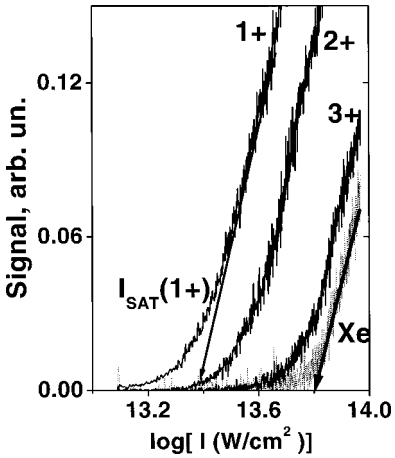


FIG. 5. Determination of the saturation intensity $I_{\mathrm{sat}}$, a molecular property relating to the response in a strong nonresonant field. A linear extrapolation to the baseline defines $I_{\mathrm{sat}}$ for the ion of interest. The calibrated absolute intensity scale is determined using the known saturation intensities for rare gas atoms such as Xenon which can be accurately fit to ADK tunneling theory.

$$S=\alpha\pi R^2 nl\phi\int_0^{I_0}\frac{1-e^{-W(I)\tau}}{I}dI, \tag{3.1}$$

where $n$ is the concentration of the neutrals, $l$ the length of the cylinder projected onto the detector, $\alpha$ the instrument sensitivity and $\phi$ is the ionization branching ratio. $W(I)$ is the intensity dependent ionization rate and $\tau$ is the effective duration of an equivalent square laser pulse. As long as $W(I)$ increases sufficiently rapidly with $I$, a simple limiting behavior obtains. In the $W(I)\gg1$ limit, the above equation leads to

$$S(I_0)=\alpha\pi R^2 nl\phi[\ln(I_0)+\ln(I_{\mathrm{sat}})], \tag{3.2}$$

where $I_{\mathrm{sat}}$ is defined to be the saturation intensity. It can be seen that $I_{\mathrm{sat}}$ is the intercept of a linear extrapolation in a plot of ion signal intensity $S$ versus $\ln I$. Importantly, $I_{\mathrm{sat}}$ is a *molecular* property which indicates the ease of ionization in a laser field of given intensity and wavelength. For example, if the ionization rate followed a power law, $W(I)=\sigma_n I^n$, the quantity $I_{\mathrm{sat}}$ would correspond to the constant intensity at which 43% of the molecules are ionized. Therefore, $I_{\mathrm{sat}}$ allows for the unambiguous characterization of the strong field molecular response as a function of wavelength and molecular properties (e.g., length, shape etc.). We note that we expect this experimental definition of $I_{\mathrm{sat}}$ to be linearly proportional to the calculated $I_{\mathrm{sat}}$ discussed above in our driven electron-in-a-box model.

A typical example of the determination of $I_{\mathrm{sat}}$ is shown in Fig. 5 for the case of singly, doubly and triply charged decatetraene parent ions, irradiated with intense 1.45 $\mu$m femtosecond laser pulses. $I_{\mathrm{sat}}$ is given by the intercept of the linear extrapolation of a plot of signal versus the log of the laser intensity. All values of $I_{\mathrm{sat}}$ reported in this paper were determined in this manner.

Absolute laser intensities were also obtained in the manner described by Hankin *et al.*[38] Briefly, the experimental ionization rate $S(I)$ for atomic rare gases (here Xenon) can be fit to the highly accurate ADK model of atomic tunnel ionization. Therefore, by fixing the measured $I_{\mathrm{sat}}$ for the Xe

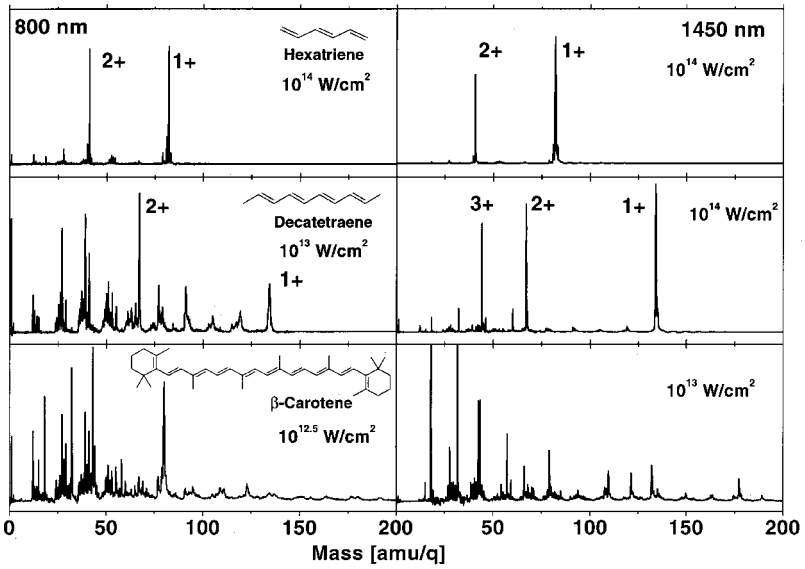


FIG. 6. Mass spectra of linear, fully conjugated all-trans hydrocarbons of increasing length: Hexatriene, decatetraene and $\beta$-carotene, using broadly tunable, intense 40 fs pulses, shown at characteristic wavelengths of 800 and 1450 nm. Hexatriene shows the formation of several charge states of the parent molecule with little fragmentation, characteristic of quasi-static tunnel ionization. The longer decatetraene shows a similar result at 1450 nm, forming singly, doubly and triply charged parent ions. Importantly, its fragmentation patterns vary with wavelength, exhibiting a transition to complete fragmentation by 800 nm. The much longer $\beta$-carotene shows extensive fragmentation at all wavelengths studied. Absolute intensities were determined using atomic Xe as a reference standard, as discussed in the text.

rare gas atom to its ADK value $[\log(I)=13.8]$, as shown in Fig. 5, the absolute intensity scale is determined. With this method, we estimate that $I_{\text{sat}}$ has an absolute error of 30% and, in the comparison of different wavelengths, a relative error of less than 20%.

## IV. EXPERIMENTAL RESULTS

In order to study the effects of delocalized electron path lengths on strong field ionization processes, we have chosen three linear unsaturated hydrocarbons with similar electronic structures (delocalized $\pi$ systems) but different effective lengths $L$: *Trans-hexatriene* (7.2 Å), *all trans-decatetraene* (13.5 Å) and *$\beta$-carotene* (32 Å). In Fig. 6 we show strong field ionization TOF mass spectra of hexatriene (HT), decatetraene (DT) and $\beta$-carotene ($\beta$C) at two different wavelengths: 0.8 and 1.45 $\mu$m. For HT, the mass spectra obtained with $I\sim10^{14}$ W/cm$^2$ at 0.8 and 1.45 $\mu$m are very similar. Both show large singly- and doubly-charged parent ions signals with very little or no fragmentation. This shows that the doubly ionized state of the HT cation is stable and that essentially no electronically excited states of the cation are formed. (It is well known that electronically excited states of cations often undergo radiationless decay processes, leading to fragmentation.[61]) Such a wavelength-independent, fragmentation-free ionization pattern, which is expected for quasistatic tunnel ionization[62] and adiabatic electron dynamics, is typical for HT over the whole range $0.8\,\mu\text{m}<\lambda<1.6\,\mu\text{m}$.

At $I\sim10^{14}$ W/cm$^2$ and $\lambda=1.45\,\mu$m, DT also yields mass spectra which are characteristic of quasistatic tunnel ionization: Singly-, doubly-, and triply-charged parent ions with little fragmentation. By contrast, at 0.8 $\mu$m DT fragments very strongly at a much lower intensity of $I\sim10^{13}$ W/cm$^2$. There is a dramatic change in the nature of the strong field ionization dynamics in DT between 1.45 and 0.8 $\mu$m. A new type of wavelength dependent ionization-fragmentation mechanism is seen in the longer DT but not in the shorter HT. This wavelength dependence of the DT ionization clearly demonstrates that any quasistatic picture fails: The electron dynamics simply cannot be adiabatic. Therefore, we have observed the transition as a function of wavelength—or, equivalently, as a function of the molecular ''length''—from quasi-static tunnel ionization to a nonadiabatic ionization dynamics. It is very important to note, as discussed in a later section, that the differences in these mass spectra cannot originate from optical resonances because, due to the large AC Stark shifts involved ($\sim$10 eV), the discrete level structure of the field-free molecule is irrelevant. The 1.4 $\mu$m mass spectrum demonstrates that even the triply charged parent ion is stable and therefore the extensive fragmentation observed at 0.8 $\mu$m is likely due to electronically excited states of the (singly and multiply charged) cation which fragment after the 40 fs laser pulse is over. This gives us a first hint that a multi-electron excitation-ionization mechanism is involved.

If the transition to nonadiabatic strong field ionization depended on the molecular length, then we expected that a still longer molecule, $\beta$-carotene, should undergo nonadiabatic ionization even at 1.5 $\mu$m. In fact, at all intensities and wavelengths between 0.4 and 1.5 $\mu$m, $\beta$C is completely fragmented. This suggests an ionization process similar to that in DT at 0.8 $\mu$m, but very different from that in DT at 1.45 $\mu$m and HT at all wavelengths, is operative.

In sum, the results of Fig. 6 demonstrate a failure of the quasi-static tunneling model for molecular ionization and suggest the onset of a nonadiabatic excitation-ionization mechanism. The failure of the quasi-static approach is seen to depend on important molecular properties such as delocalized electron path lengths.

We consider two possibilities for the large energy absorption in the field which leads to the extensive fragmentation of DT seen in Fig. 6 at 0.8 $\mu$m. One is that a single active electron (SAE) experiences extensive above threshold ionization–absorption (ATI),[54] reaching a superexcited state of the cation which subsequently decays, leading to the observed fragmentation after the laser pulse is over. The other possibility is that multiple active electrons (MAE) each absorb energy from the laser field to form complex multiply

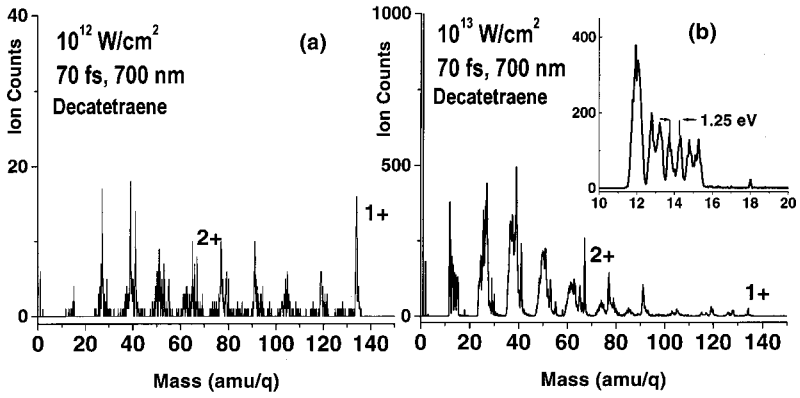


FIG. 7. Mass spectra of all-trans decatetraene at high and low laser intensities, using 700 nm, 70 fs pulses. At the detection threshold intensity of $10^{12}$ W/cm$^2$ (yielding about 1 ion per 250 laser shots), the fragmentation is as extensive as at $10^{13}$ W/cm$^2$. The fragments shows significant kinetic energy release. Inset: The methyl group part of the mass spectrum (12–15 amu). The forward–backward splitting corresponds to $CH_3$ fragment average energies of 1.25 eV and highly directional emission, uncharacteristic of typical unimolecular decomposition processes in photoexcited ions.

excited states of the ion core which also decay after the laser pulse is over. We expect these two processes to have very different intensity dependencies. The SAE ATI case should have a very high order intensity dependence (i.e., one electron must coherently absorb many photons) as compared with the MAE case.

In Fig. 7, we show DT ionization-fragmentation patterns for 70 fs, 0.7 $\mu$m irradiation at intensities of $I\sim10^{12}$ and $I\sim10^{13}$ W/cm$^2$. It can be seen that even at this lowest laser intensity where ionization signals can just be observed, $10^{12}$ W/cm$^2$ [Fig. 7(a), 1 count per 200–300 laser shots], the fragmentation is as severe as at $10^{13}$ W/cm$^2$ [Fig. 7(b)] where the ionization rate is much higher. The route to ionization for DT at 0.7 $\mu$m appears the same at $10^{12}$ W/cm$^2$ as at $10^{13}$ W/cm$^2$. This result cannot be reconciled with a model based on SAE above threshold ionization because the highly nonlinear behavior of ATI with intensity would yield much less fragmentation at the lower intensity. This result indicates that multiple active electrons are involved in the strong field ionization. Therefore, we suggest that the new ionization dynamics seen in DT at 0.8 $\mu$m is a nonadiabatic multi-electron (NME) excitation-ionization process.

It is interesting to analyze further the DT fragments shown in Fig. 7(b). In a linear TOFMS,[63] it is possible to determine the kinetic energy $E_{\mathrm{kin}}$ released during the fragmentation from the "turn-around time" splitting $\Delta t$ seen in fragment ion mass peaks: $\Delta t=\sqrt{mE_{\mathrm{kin}}/qF_{\mathrm{acc}}}$ (where $F_{\mathrm{acc}}$ is the extraction field applied to ions of charge $q$ and mass $m$). We find that at $I\sim10^{13}$ W/cm$^2$ the kinetic-energy release in the fragments is considerably larger than expected for simple photochemical bond cleavage in polyatomic molecules. The inset in Fig. 7(b) demonstrates that the 13–15 amu ($CH_x$, $x=1-3$) peak shapes correspond to an average kinetic-energy release of 1.25 eV. Furthermore, the clear double peak structure shows that the dissociation is highly directional, in contradiction with simple bond rupture unimolecular decay[64] where isotropic emission is expected. As noted above, the large aperture mass spectrometer used in this measurement did not vignette the ion trajectories. Our analysis of the peak shapes for the $C_2^+$ and $C_3^+$ fragments indicates average (maximal) kinetic energies of 2 eV (4.2 eV) and 0.9 eV (3 eV), respectively. While these kinetic energies are well below those typically observed in intense-field Coulomb explosion ($I\sim10^{15}$ W/cm$^2$) of multiply charged molecular ions,[36,43] they are much higher than those expected for typical unimolecular decomposition of photoexcited ions.[61] The C–C sigma bond fission processes observed here are generally slow compared to a 40 fs laser pulse. In sum, these results suggest that multielectron excitation leads to an electronically excited, multiply charged parent ion which subsequently fragments, partially assisted by some Coulombic repulsion.

Through the saturation intensity $I_{\mathrm{sat}}$ (as explained in Sec. III), it is possible to determine the intensity dependent ionization/fragmentation of DT as a function of wavelength. This approach reveals further insight into the strong field molecular response. In Fig. 8, we show the measured $I_{\mathrm{sat}}$ for HT (80 amu), DT (134 amu) and the DT-fragments, at 0.8 and 1.5 $\mu$m. We can see that $I_{\mathrm{sat}}$ for HT is wavelength independent, consistent with quasistatic tunnel ionization. It can be seen that for the 0.8 $\mu$m case, DT fragments (triangles) in the 78–120 amu range, corresponding to singly charged $C_9$, $C_8$, $C_7$, and $C_6$ fragments, have all approximately the same $I_{\mathrm{sat}}$ of $1.1\times10^{13}$ W/cm$^2$. This value is very close to that of the DT parent ion $I_{\mathrm{sat}}$ at 0.8 $\mu$m. This result once again points towards a NME excitation–ionization process, where the fragmentation process cannot be separated from ionization.

For the case of the formation of some smaller fragments such as $C_2H_5^+$, the saturation intensity ($I_{\mathrm{sat}}\approx1.8\times10^{13}$ W/cm$^2$) remains relatively close to that of the parent ion. Nevertheless, at 0.8 $\mu$m, for fragments smaller than $C_6H_n$, the response appears more structured, depending on the number of hydrogen losses for each carbon group. For example, in the case of $C_2H_n^+$ with $n=0\cdots7$, $I_{\mathrm{sat}}$ varies between $1.8\times10^{13}$ and $4.5\times10^{13}$. It should be noted that for such small fragments only 1 to 2 $\pi$-bonding orbitals are remaining in the fragment. Therefore, C–C bond fission should be energetically favorable compared to hydrogen atom loss. The saturation intensity for DT double ionization is very close to those of the fragments smaller than $C_6$ which have lost more than one hydrogen. As the doubly- and triply-charged DT parent ions are themselves stable, this result suggests that the multiple hydrogen loss channels are caused mainly by the formation of electronically excited, multiply-charged parent ions.

Although the fragmentation yield of DT at 1.5 $\mu$m is

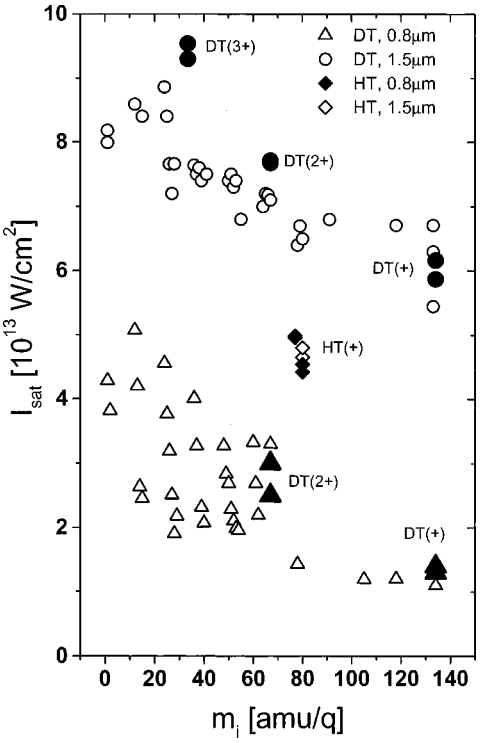


FIG. 8. Saturation intensities $I_{sat}$ for different fragment ions of mass $m_i$ of the parent molecule decatetraene (DT), obtained at two different wavelengths: 0.8 $\mu$m (triangles) and 1.5 $\mu$m (circles). Also included are the $I_{sat}$ determined for multiply charged parent ions (big symbols), and for Hexatriene (HT) at both 0.8 $\mu$m (black diamonds) and 1.4 $\mu$m (white diamonds). For a discussion, see the text.

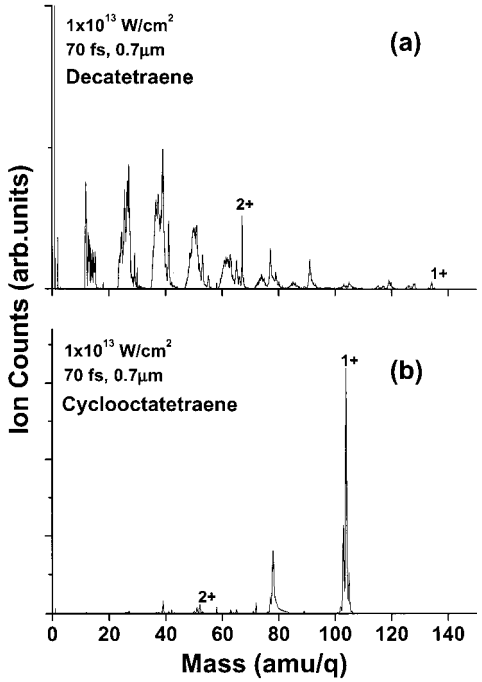


FIG. 9. Time of flight mass spectra for all-trans Decatetraene (DT) and Cylcooctatetraene (COT), obtained using a 700 nm, 70 fs laser pulse. While COT shows little fragmentation and almost no doubly charged states, DT (with the same number of $\pi$-bonds) fragments severely due to the much longer delocalized electron path length in the direction of the laser field (see text).

very small as compared to the yield of multiply (2+, 3+) charged parent ions (see Fig. 6), $I_{sat}$ can be determined for these fragments nonetheless. In contrast to the destructive ionization seen at 0.8 $\mu$m, at 1.5 $\mu$m $I_{sat}$ for the DT-fragments generally occurs at higher intensities than $I_{sat}$ of the parent DT ion. Reaching $I_{sat}$ for the fragments requires quite high intensities. Additionally, the hydrogen loss channels for each fragment group $C_n$ appears to be less dominant. We also note that the fragment mass peak shapes are generally sharper at 1.5 $\mu$m than at 0.8 $\mu$m, suggesting that there is much less kinetic-energy release amongst the fragments (see Fig. 6). We suggest that at 1.5 $\mu$m most of the DT fragments are formed in a more typical statistical unimolecular fragmentation process which occurs long after the laser pulse. This can still be reconciled with a quasi-static tunnel ionization picture provided that the quantitative stabilities of the multiply charged parent ions are known. Unfortunately, to the best of our knowledge, there exists no experimental data on the breakdown behavior of DT upon excitation–ionization. A detailed study, using conventional techniques such as electron impact ionization, would help to clarify this situation.

Figure 8 also includes some experimental results for the $I_{sat}$ of HT, measured at 0.8 and 1.5 $\mu$m. We find that $I_{sat} \approx 5 \cdot 10^{13}$ W/cm$^2$ and is wavelength independent. From these observations it is clear that at 0.8 $\mu$m HT has reached its corresponding long wavelength limit and that a further increase in wavelength does not significantly alter the strong field ionization response.

It is interesting to compare the strong field electronic response of the quasilinear DT molecule to its cyclical counterpart cylcooctatetraene (COT). Both molecules have the same number of delocalized $\pi$ electrons, very similar numbers of vibrational degrees of freedom and approximately the same $I_p$. Simple quasistatic tunneling models would therefore suggest that they ionize in similar ways. Figure 9 shows a comparison of the mass spectra of DT and COT under $10^{13}$ W/cm$^2$ irradiation at 0.7 $\mu$m. While COT shows little fragmentation and a very strong parent ion signal, DT is almost completely fragmented, with a broad distribution between $CH_x$ and $C_7H_x$. Again, the extensive kinetic-energy release in the DT fragments suggests that electronically excited multiply charged states of the cation are formed during the laser pulse, consistent with NME dynamics. Although unimolecular decay rates of ring compounds are generally expected to be slower than those of their linear analogues (two bonds need to be broken), these results show that COT does not even form multiply charged ion states. This indicates that the delocalized electrons in COT simply do not interact as strongly with the field as those of DT. The differences in fragmentation patterns between DT and COT cannot simply be due to different length-corrected MSAE Keldysh parameters[37] because we are unable to avoid fragmentation of DT even at the lowest ionization intensities. This ''geometric'' comparison shows that the three dimensional shape of the molecule is much more influential than simply the total number of delocalized electrons. The ring geometry of COT determines that the effective path length of a delocalized electron in the direction of the laser field is

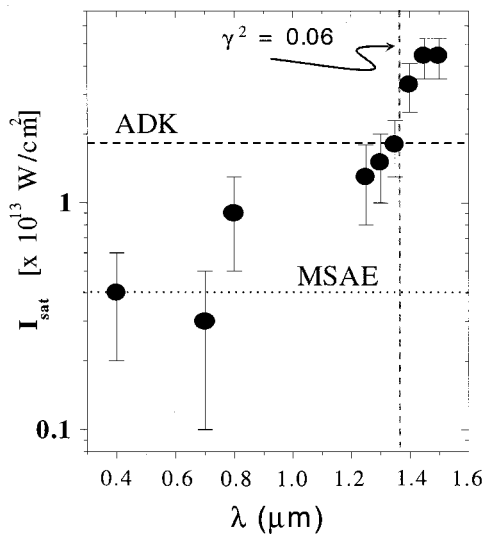


FIG. 10. The wavelength dependence of $I_{sat}$ for all-trans decatetraene shows a transition from quasi-static (wavelength independent) to NME dynamics near 0.8 $\mu$m. $I_{sat}$ increases by ~400% between 0.8 and 1.5 $\mu$m, demonstrating the failure of quasi-static models. The calibrated, absolute $I_{sat}$ were determined using Xe as a reference standard. The expectations of both atomic tunnel ionization models (ADK, dashed line) and the length-corrected molecular single active electron model (MSAE, dotted line) are shown. $I_{sat}$ significantly exceed the expectations of both the ADK and MSAE results at $\lambda \sim 1.4$ $\mu$m, due to multiple active electron effects.

quite short (as compared with DT) and, therefore, it will interact much less strongly, consistent with the observations.

In order to study the transition from adiabatic tunneling to NME ionization dynamics in further detail, we have investigated the wavelength dependence of $I_{sat}$ for the DT case. The results of this extensive study are presented in Fig. 10. For the case of adiabatic electron dynamics, implicit in all quasi-static tunnel ionization models, the $I_{sat}$ is by definition wavelength independent. Using the ionization potential appropriate to DT, we have included in Fig. 10 the ADK atomic tunnel ionization result (ADK, dashed line) and the prediction of the molecular single active electron (MSAE) tunnelling model, using the ionization potential and the length of DT (MSAE, dotted line). The MSAE model corrects the atomic result by accounting for changes in the tunnelling barrier due to the molecular length.[37] Wavelength independence is not observed, demonstrating the failure of quasi-static models. Between 1.45 and 0.8 $\mu$m $I_{sat}$ decreases by a factor of 4 to 5, which implies a very dramatic increase in the (highly nonlinear) ionization rate towards shorter wavelengths. We find that a wavelength-independent $I_{sat}(\lambda)$ is achieved only in the long wavelength limit of these studies, at around 1.45 $\mu$m. This is fully consistent with the concomitant reduction in DT fragmentation at 1.45 $\mu$m shown in Fig. 6. As the wavelength decreases, the molecule becomes much easier to ionize and, simultaneously, the fragmentation channels grow extensively, completely dominating by 0.8 $\mu$m (Fig. 6).

Most importantly, the departure from quasi-static tunneling can occur even when the Keldysh parameter $\gamma$ is less than unity, whether corrected or not for molecular size effects.[37] For DT, the departure from adiabatic (wavelength independent) behavior starts at $\gamma^2 \sim 0.06$ (without molecular size corrections which would further reduce its value). This value is traditionally considered to be in the tunneling regime. This clearly indicates that the Keldysh parameter cannot be used as a simple diagnostic of quasistatic tunnelling behavior in polyatomic molecules. A consideration of the electron dynamics inside the molecule becomes important.

It is also important to note that this transition from quasi-static to NME ionization dynamics cannot be interpreted as a consequence of resonant photon absorption, as would be natural in the perturbative limit. Indeed, at these laser intensities, the voltage $\mathcal{E}L$ applied by the laser field across the molecule approaches the ionization potential $I_p \sim 10$ eV. In such cases, the AC Stark shifts of *delocalized* molecular orbitals approach $I_p$ (i.e., every optical cycle, the bound electronic states sweep through ~10 eV) and the discrete level structure which governs energy absorption in weak laser fields becomes irrelevant.

Figure 10 dramatically illustrates the transition from quasi-static to NME dynamics. Interestingly, it also demonstrates the importance of multi-electron effects even in the long-wavelength limit where quasistatic behavior obtains. It can clearly be seen that the experimental long-wavelength limit $I_{sat}$ is significantly higher than *both* the ADK and MSAE values. We believe that this increase in the quasi-static $I_{sat}$ must be due to multi-electron effects that originate in the dynamic polarization of all delocalized electrons in the strong field. As a consequence, via Coulomb interactions, these polarized electrons repel the active electron and effectively increase the tunnelling barrier for the 'active' electron and therefore leads to a larger value of $I_{sat}$. We are presently carrying out an experimental investigation into the nonresonant (IR) strong field ionization of neutral metal clusters. As metal clusters have a short length but many equivalent highly polarizable electrons, they represent ideal systems for the investigation of these dynamic multielectron polarization effects in the long-wavelength limit. The results of these studies will be reported in a future publication.

## V. CONCLUSION

The quasi-static model of strong field ionization, highly successful in atomic physics, is based upon two fundamental assumptions. The first is the adiabatic approximation that the time scale of electron motion inside the binding potential well is much faster than the laser period, allowing the neglect of any electron dynamics inside the atom and/or molecule, often justified by the small size of rare gas atoms. The second is that only a single active electron (SAE) is operational, justified because the doubly excited states which contribute to the polarizability lie above the ionization potential in rare gas atoms. Our studies were motivated by two concerns. Firstly, that as the path lengths of delocalized electrons gets longer in molecules, the adiabatic approximation may fail and the driven electron dynamics inside the molecule will become important. Secondly, that the neglect of multiple active electrons (MAE) is not easily justified in molecules, as doubly excited states often exist below the ionization potential.

We studied the nonresonant strong field ionization of a series of linear unsaturated hydrocarbons (HT, DT, and $\beta$C) as a function of intensity and wavelength, using mass spectrometry. We specifically used short ~40 fs laser pulses in order to avoid (i) domination by vibrationally induced dynamic electron localization effects (such as enhanced ionization) or (ii) field-induced alignment effects during the interaction. This allowed us to emphasize the purely electronic response to the field. A restricted collection volume TOFMS ensured that observed ion signals originated from a cylinder of constant axial intensity. This allowed us to make calibrated absolute intensity measurements as a function of wavelength, based on the saturation intensity $I_{sat}$. We observed and characterized a new type of strong field molecular behavior: Nonadiabatic multi-electron (NME) excitation-ionization dynamics.

We observed that the onset of NME ionization depends on the time scale (path length) of delocalized electron motion as compared with the laser period. In HT behavior consistent with quasistatic tunnel ionization was observed at all wavelengths. In DT we observed the transition as a function of wavelength from quasistatic tunnel ionization to NME ionization. In $\beta$C NME ionization was observed at all wavelengths. Our study showed that the saturation intensity $I_{sat}$ in DT varied by over 400% in the 0.8–1.5 $\mu$m range, demonstrating a complete failure of the adiabatic approximation. The inherently multi-electron nature of the interaction was corroborated by studies of (i) intensity effects on fragmentation patterns and (ii) kinetic energy distributions amongst the fragments. We emphasized that the popular Keldysh parameter, often used as a diagnostic of tunneling behavior, becomes meaningless when electron dynamics inside the molecule become important.

The SAE assumption in the (adiabatic limit) quasi-static tunneling of molecules has also been questioned. Even in the long wavelength quasistatic limit for DT (around 1.5 $\mu$m), multi-electron effects were observed. The experimental $I_{sat}$ in this limit was higher than the atomic ADK expectation and significantly higher than the length-corrected molecular single active electron MSAE expectation. We suggest that this is due to the dynamic polarization of all electrons in the molecule which, via Coulomb repulsion, effectively increasing the tunnelling barrier for the active electron.

In order to gain an intuitive picture of NME dynamics, we developed a very simple driven electron-in-a-box model, similar to that used in clusters studies.[53] While most qualitative features of the physics were reproduced, supporting our picture, a time-dependent multi-configuration Hartree–Fock or density functional model needs to be developed in order to proceed further. We note that our physical model is also consistent with and is supported by another recent experiment.[65]

The emergence of NME ionization dynamics in delocalized electron systems will have important consequences for many applications of intense laser pulses. A recently proposed mechanism of strong-field control in polyatomic molecules[12] is based on effective broadening of all states, making them energetically accessible without tuning to field-free resonances. We believe that the highly efficient nonresonant nonadiabatic multielectron processes described in this paper are a clear manifestation of and a physical mechanism for such broadening. In fs-mass spectrometry, NME dynamics can lead to almost complete fragmentation of the parent ion, even at threshold ionization intensities. In fs laser machining, dynamic polarization effects will directly affect damage thresholds. Conceptually, NME ionization dynamics bridges the gap between atomic strong field ionization and the panoply of strong field phenomena observed in larger molecules, clusters and solids. In intense field coherent control, the nature of the driven electron response will be strongly affected by NME dynamics. Below the ionization threshold, NME should allow for the highly efficient excitation of various multi-electron states which are inaccessible via conventional means. This may lead to new avenues for the control of unimolecular reaction dynamics. Consequently, we expect that an area of future investigation will be the effects of pulse shape (e.g., chirp) on intense field NME dynamics and its potential or lack thereof for the optical control of molecular processes.

## ACKNOWLEDGMENTS

It is a pleasure to acknowledge valuable contributions from P. Arya and M. Barnes for the synthesis of all trans-decatetraene and D.M. Rayner, D.M. Villeneuve, and S. Hankin for technical assistance. We have benefited greatly from stimulating discussions with many colleagues including P.B. Corkum, S. Hankin, D.M. Rayner, D.M. Villeneuve, M.Z. Zgierski, and H.G. Muller. M.I. acknowledges stimulating discussions with R. Levis and A. Markevitch. M.L. and V.B. thank the NSERC Visiting Fellowships Program for financial support. M.L. also thanks the Austrian Fund for the Advancement of Science (FWF).

[1] A. Baltuska, Wei Zhiyi, M. S. Pshenichnikov, and D. A. Wiersma, Opt. Lett. **22**(2), 102 (1997); A. Baltuska, Z. Wei, M. S. Pshenichnikov, D. A. Wiersma, and R. Szipocs, Appl. Phys. B: Lasers Opt. **65**(2), 175 (1997).
[2] A. Stingl, M. Lenzner, C. Spielmann, F. Krausz, and R. Szipocs, Opt. Lett. **20**(6), 602 (1995); M. Nisoli, S. Stagira, S. De-Silvestri, O. Svelto, S. Sartania, Z. Cheng, M. Lenzner, C. Spielmann, and F. Krausz, Appl. Phys. B: Lasers Opt. **65**(2), 189 (1997); S. Sartania, Z. Cheng, M. Lenzner, G. Tempea, Ch. Spielmann, and F. Krausz, Opt. Lett. **22**(20), 1562 (1997).
[3] G. Steinmeyer, D. H. Sutter, L. Gallmann, N. Matuschek, and U. Keller, Science **286**, 327(5444) (1999).
[4] H. Wang, S. Backus, Z. Chang *et al.*, J. Opt. Soc. Am. B **16**, 1790 (1999); S. Backus, C. G. Durfee III, M. M. Murnane, and H. C. Kapteyn, Rev. Sci. Instrum. **69**, 1207 (1998).
[5] A. L'Huillier and Ph. Balcou, Phys. Rev. Lett. **70**, 774 (1993).
[6] J. J. Macklin, J. D. Kmetetc, and C. L. Gordon III, Phys. Rev. Lett. **70**, 766 (1993).
[7] C. Spielmann, H. Burnett, R. Sartania, R. Koppitsch, M. Schnurer, C. Kan, M. Lenzner, P. Wobrauschek, and F. Krausz, Science **278**, 661 (1997).
[8] K. W. D. Ledingham and R. P. Singhal, Int. J. Mass Spectrom. Ion Processes **163**(3), 149 (1997); N. P. Lockyer and J. C. Vickerman, *ibid.* **176**(1–2), 77 (1998); S. Pedersen and A. H. Zewail, Mol. Phys. **89**(5), 1455 (1996).
[9] See, e.g., *Laser Ablation, Proceedings of the 5th International Conference*, edited by J. S. Horwitz, H. U. Krebs, K. Murakami, and M. Stuke, Appl. Phys. A: Mater. Sci. Process. (Springer, New York, 1999).
[10] See, e.g., K. Miura *et al.*, Appl. Phys. Lett. **71**, 3329 (1997).
[11] See, e.g., A. Assion, T. Baumert, M. Bergt, T. Brixner, B. Kiefer, V. Seyfried, M. Strehle, and G. Gerber, Science **282**, 919 (1998); B. Sheehy and L. F. DiMauro, Annu. Rev. Phys. Chem. **47**, 463 (1996); T. C. Weinacht, J. L. White, and P. H. Bucksbaum, J. Phys. Chem. A **103**, 10166 (1999).
[12] R. J. Levis, G. M. Menkir, and H. Rabitz, Science **292**, 709 (2001).
[13] A. D. Bandrauk, S. Chelkowski, and P. B. Corkum, Int. J. Quantum Chem.

**75**(4–5), 951 (1999); S. Chelkowski, P. B. Corkum, and A. D. Bandrauk, Phys. Rev. Lett. **82**, 3416 (1999); H. Stapelfeldt, E. Constant, H. Sakai, and P. B. Corkum, Phys. Rev. A **58**, 426 (1998).
[14] J. P. Nibarger, S. V. Menon, and G. N. Gibson, Phys. Rev. A **63**, 053406 (2001); G. N. Gibson, M. Li, C. Guo, and J. P. Nibarger, *ibid.* **58**, 4723 (1998); C. Guo, M. Li, and G. N. Gibson, Phys. Rev. Lett. **82**, 2492 (1999).
[15] S. Augst, D. Strickland, D. D. Meyerhofer, S. L. Chin, and J. H. Eberly, Phys. Rev. Lett. **63**(20), 2212 (1989).
[16] B. Walker, B. Sheehy, L. F. DiMauro, P. Agostini, K. J. Schafer, and K. C. Kulander, Phys. Rev. Lett. **73**(9), 1227 (1994).
[17] P. B. Corkum, Phys. Rev. Lett. **71**, 1994 (1993).
[18] H. G. Muller, Phys. Rev. A **60**(2), 1341 (1999).
[19] M. J. Nandor, M. A. Walker, L. D. Van-Woerkom, and H. G. Muller, Phys. Rev. A **60**, R1771 (1999).
[20] A. Talebpour, S. Larochelle, and S. L. Chin, J. Phys. B **31**, L49 (1998); **31**, 2769 (1998); F. A. Ilkov, J. E. Decker, and S. L. Chin, *ibid.* **25**, 4005 (1992).
[21] L. V. Keldysh, Zh. Eksp. Teor. Fiz. **47**, 1945 (1964) [Sov. Phys. JETP **20**, 1307 (1965)].
[22] F. H. M. Faisal, J. Phys. B **6**, L89 (1973).
[23] H. R. Reiss, Phys. Rev. A **22**, 1786 (1980).
[24] A. M. Perelomov, V. S. Popov, and M. V. Terent'ev, Zh. Eksp. Teor. Fiz. **50**, 1393 (1966) [Sov. Phys. JETP **23**, 924 (1966)]; **51**, 309 (1966); [**24**, 207 (1967)]; A. M. Perelomov and V. S. Popov, *ibid.* **52**, 514 (1967) [**25**, 336 (1967)]; V. S. Popov, V. P. Kuznetsov, and A. M. Perelomov, *ibid.* **53**, 331 (1967) [*ibid.* **26**, 222 (1968)].
[25] M. V. Ammosov, N. D. Delone, and V. P. Kraïnov, Sov. Phys. JETP **64**, 1191 (1986); N. B. Delone and V. P. Kraïnov, J. Opt. Soc. Am. B **8**, 1207 (1991); V. P. Kraïnov and V. M. Ristić, Sov. Phys. JETP **74**, 789 (1992).
[26] T. Weber, H. Giessen, M. Weckenbrock *et al.*, Nature (London) **405**(6787), 658 (2000).
[27] B. Yang, M. Pont, R. Shakeshaft, E. van-Duijn, and B. Piraux, Phys. Rev. A **56**(6), 4946 (1997).
[28] K. C. Kulander, Prog. Cryst. Growth Charact. Mater. **33**(1–3), 193 (1996); K. J. Schafer and K. C. Kulander, Phys. Rev. A **42**(9), 5794 (1990); B. Yang, K. J. Schafer, B. Walker, K. C. Kulander, L. F. DiMauro, and P. Agostini, Acta Phys. Pol. A **86**(1–2), 41 (1994).
[29] H. Yu and A. D. Bandrauk, J. Chem. Phys. **102**, 1257 (1995).
[30] T. Seideman, M. Ivanov, and P. Corkum, Phys. Rev. Lett. **75**, 2819 (1995).
[31] T. Zuo and A. D. Bandrauk, Phys. Rev. A **52**, R2511 (1995); S. Chelkowski, A. Conjusteau, T. Zuo, and A. D. Bandrauk, *ibid.* **54**, 3235 (1996).
[32] Hengtai Yu and A. D. Bandrauk, Phys. Rev. A **56**, 685 (1997); I. Last and J. Jortner, *ibid.* **58**, 3826 (1998).
[33] I. Kawata, H. Kono, Y. Fujimura, and Andr D. Bandrauk, Phys. Rev. A **62**, 031401 (2000).
[34] E. Constant, H. Stapelfeldt, and P. B. Corkum, Phys. Rev. Lett. **76**(22), 4140 (1996); C. Ellert and P. B. Corkum, Phys. Rev. A **59**(5), R3170 (1999).
[35] D. Normand, M. Schmidt, Phys. Rev. A **53**(4), R1958 (1996).
[36] See, e.g., L. J. Frasinski, K. Codling, and P. A. Hatherly, Science **246**, 1029 (1989); L. J. Frasinski, K. Codling, P. Hatherly, I. Barr, I. N. Ross, and W. T. Toner, Phys. Rev. Lett. **58**, 2424 (1987); D. T. Strickland, Y. Beaudoin, P. Dietrich, and P. B. Corkum, *ibid.* **68**, 2755 (1992); M. Schmidt, D. Normand, and C. Cornaggia, Phys. Rev. A **50**, 5037 (1994).
[37] R. J. Levis and M. J. DeWitt, J. Phys. Chem. A **103**(33), 6493 (1999); B. S. Prall, M. J. DeWitt, and R. J. Levis, J. Chem. Phys. **111**(7), 2865 (1999); M. J. DeWitt and R. J. Levis, *ibid.* **110**(23), 11368 (1999); M. J. DeWitt and R. J. Levis, Phys. Rev. Lett. **81**(23), 5101 (1998).
[38] S. M. Hankin, D. M. Villeneuve, P. B. Corkum, and D. M. Rayner, Phys. Rev. Lett. **84**(22), 5082 (2000); Phys. Rev. A **64**, 013405 (2001).
[39] C. Wulker, W. Theobald, D. Ouw, F. P. Schafer, and B. N. Chichkov, Opt. Commun. **112**(1–2), 21 (1994); U. Teubner, C. Wulker, W. Theobald, and E. Forster, Phys. Plasmas **2**(3), 972 (1995).
[40] S. Hunsche, T. Starczewski, A. l'Huillier, A. Persson, C. G. Wahlstrom, B. Van Linden Van Den Heuvell, and S. Svanberg, Phys. Rev. Lett. **77**(10), 1966 (1996).
[41] M. Tchaplyguine, K. Hoffmann, O. Duhr, H. Hohmann, G. Korn, H. Rottke, M. Wittmann, I. V. Hertel, and E. E. B. Campbell, J. Chem. Phys. **112**(6), 2781 (2000).
[42] G. Helden, I. Holleman, G. M. H. Knippels, A. F. G. van der Meer, and G. Meijer, Phys. Rev. Lett. **79**(26), 5234 (1997); G. Helden, I. Holleman, and G. Meijer, Opt. Express **4**, 2 (1999).
[43] J. Purnell, M. Snyder, S. Wei, and A. W. Castleman, Jr., Chem. Phys. Lett. **229**, 333 (1994); E. M. Snyder, S. Wei, J. Purnell, S. A. Buzza, A. W. Castleman, Jr., *ibid.* **248**, 1 (1996).
[44] L. Koller, M. Schumacher, J. Kohn, S. Teuber, J. Tiggesbaumker, K. H. Meiwes-Broer, Phys. Rev. Lett. **82**(19), 3783 (1999); S. Teuber, T. Doppner, M. Schumacher, J. Tiggesbaumker, and K. H. Meiwes-Broer, Aust. J. Phys. **52**(3), 555 (1999); T. Doppner, S. Teuber, M. Schumacher, J. Tiggesbaumker, and K. H. Meiwes-Broer, Int. J. Mass. Spectrom. **192**, 387 (1999); M. Schumacher, S. Teuber, L. Koller, J. Kohn, J. Tiggesbaumker, and K. H. Meiwes-Broer, Eur. Phys. J. D **9**(1–4), 411 (1999).
[45] T. Ditmire, J. W. G. Tisoh, E. Springate, M. B. Mason, N. Hay, R. A. Smith, J. Marangos, and M. H. R. Hutchinson, Nature (London) **386**(6620), 54 (1997); T. Ditmire, J. W. G. Tisch, E. Springate, M. B. Mason, N. Hay, J. P. Marangos, and M. H. R. Hutchinson, Phys. Rev. Lett. **78**(14), 2732 (1997).
[46] J. W. G. Tisch, T. Ditmire, D. J. Fraser, N. Hay, M. B. Mason, E. Springate, J. P. Marangos, and M. H. R. Hutchinson, J. Phys. B **30**(20), L709 (1997).
[47] See, e.g., J. D. Kmetec, C. L. Gordon III, J. J. Macklin, B. E. Lemoff, G. S. Brown, and S. E. Harris, Phys. Rev. Lett. **68**, 1527 (1992); A. McPherson, B. D. Thompson, A. B. Borisov, K. Boyer, and C. K. Rhodes, Nature (London) **370**, 6491 (1994); S. Dobosz, M. Lezius, M. Schmidt, P. Meynadier, M. Perdrix, D. Normand, J. P. Rozet, and D. Vernhet, Phys. Rev. A **56**(4), R2526 (1997).
[48] M. Lezius, S. Dobosz, D. Normand, and M. Schmidt, Phys. Rev. Lett. **80**(2), 261 (1998); M. Lezius, S. Dobosz, D. Normand, and M. Schmidt, J. Phys. B **30**(7), L251 (1997).
[49] C. Rose-Petruck, K. J. Schafer, K. R. Wilson, and C. P. J. Barty, Phys. Rev. A **55**(2), 1182 (1997).
[50] Y. L. Shao, T. Ditmire, J. W. G. Tisch, E. Springate, J. P. Marangos, and M. H. R. Hutchinson, Phys. Rev. Lett. **77**(16), 3343 (1996).
[51] E. Springate, N. Hay-N, J. W. C. Tisch, M. B. Mason, T. Ditmire, M. H. R. Hutchinson, and J. P. Marangos, Phys. Rev. A **61**(6), 063201/1 (2000); T. Ditmire, E. Springate, J. W. G. Tisch, Y. L. Shao, M. B. Mason, N. Hay, J. P. Marangos, and M. H. R. Hutchinson, *ibid.* **57**(1), 369 (1998).
[52] M. Lezius, V. Blanchet, D. M. Rayner, D. M. Villeneuve, A. Stolow, and M. Yu. Ivanov, Phys. Rev. Lett. **86**, 51 (2001).
[53] V. Veniard, R. Taieb, and A. Maquet, Phys. Rev. A **60**, 3952 (1999).
[54] See, e.g., N. B. Delone and V. P. Krainov, *Atoms in Strong Light Fields* (Springer Ser. Chem. Phys., New York, 1985), Chap. 4, Vol. 28.
[55] See, e.g., A. D. Bandrauk, E. Aubanel, and J.-M. Gauthier, in *Molecules in Laser Fields*, edited by A. D. Bandrauk (Marcel Dekker, New York, 1994), Chap. 3.
[56] See, e.g., C. Wunderlich, E. Kobler, H. Figger, and T. W. Hnsch, Phys. Rev. Lett. **78**, 2333 (1997); J. W. J. Verschuur, L. D. Noordam, and H. B. van Linden van den Heuvell, Phys. Rev. A **40**, 4383 (1989).
[57] R. S. Mulliken, J. Chem. Phys. **7**, 20 (1939).
[58] D. A. Harmin, Phys. Rev. A **56**(1), 232 (1997); **44**(1), 433 (1991); D. A. Harmin and P. N. Price, *ibid.* **49**(3), 1933 (1994); M. J. Cavagnero and S. T. Cornett, *ibid.* **55**(5), 3746 (1997).
[59] H. B. van-Linden-van-den-Heuvell, R. Kachru, N. H. Tran, and T. F. Gallagher, Phys. Rev. Lett. **53**(20), 1901 (1984); T. F. Gallagher, Comments At. Mol. Phys. **30**(4), 221 (1994); M. Gatzke, R. B. Watkins, and T. F. Gallagher, Phys. Rev. A **51**(6), 4835 (1995).
[60] I. Fischer, M. J. J. Vrakking, D. M. Villeneuve, and A. Stolow, Chem. Phys. **207**, 331 (1996).
[61] See, e.g., T. E. Carney and T. Baer, J. Chem. Phys. **76**, 5968 (1982).
[62] H. Sakai, H. Stapelfedt, E. Constant, M. Yu Ivanov, D. R. Matusek, J. S. Wright, and P. B. Corkum, Phys. Rev. Lett. **81**(11), 2217 (1998).
[63] W. C. Wiley and I. H. McLaren, Rev. Sci. Instrum. **26**, 12 (1955).
[64] E. F. Cromwell, A. Stolow, M. J. J. Vrakking, and Y. T. Lee, J. Chem. Phys. **97**, 4029 (1992).
[65] A. N. Markevitch, N. P. Moore, and R. J. Levis, Chem. Phys. **267**(1–3), 131 (2001).